ISSN: 0973-4929, Vol. 20, No. (3) 2025, Pg. 1253-1264

Current World Environment

www.cwejournal.org

Photocatalytic Degradation of Bismarck Brown Y azo dye by using an Immobilised Photocatalyst and their Reusability

CHHATAR PAL, SHANKER LAL MEENA* and ASHUTOSH SHARMA

Department of Chemistry, Jai Narain Vyas University, Jodhpur, Rajasthan, India.

Abstract

The elimination of organic pollutants, particularly azo dyes, is of critical concern due to their toxicity, chemical stability, and mutagenic effects on living systems. In this work, the photocatalytic degradation of Bismarck Brown Y, a representative azo dye, was investigated using Amberchrom 1×2 in its chloride form, immobilized as a photocatalyst with a mesh size of 100–200, which also functions as an adsorbent. The fine mesh size provides a higher surface area, facilitating both dye adsorption and enhanced interaction with incident light, thereby improving photocatalytic activity. The degradation efficiency was systematically evaluated as a function of pH, initial dye concentration, catalyst dosage, and UV light intensity. Among the tested conditions, the highest degradation performance was obtained at 30 °C, neutral pH (7), a photocatalyst loading of 0.40 g, and an irradiation intensity of 10.5 mW cm^{-2}. Under these optimized parameters, complete degradation of the dye was achieved within 35 minutes with a degradation efficiency of 99.5%, confirming the efficiency of immobilized Amberchrom 1×2 as a potential photocatalyst for the treatment of azo dye pollutants in wastewater. The apparent rate constant (kapp) for the photocatalytic degradation under these conditions was calculated as $1.53\times10^{-1}\,min^{-1}$ ($t_{1/2}$ = 4.53 min), indicating a significant degradation rate consistent with the observed efficiency.

Article History
Received: 11 June 2025
Accepted: 11 September 2025

Keywords
Bismarck Brown Y Azo Dye;
Immobilisation;
Photocatalytic Degradation,
Photosensitizer;
Reusability.

Introduction

The discharge of dye-contaminated wastewater from various industries has emerged as a significant environmental challenge worldwide. Azo dyes, widely used in textiles, food, and cosmetics, pose persistent problems due to their complex chemical structures that render them highly resistant to conventional wastewater treatment methods such as coagulation-flocculation and biological degradation. Traditional treatments are often ineffective, as these dyes not only exhibit toxicity but also reduce light penetration in aquatic systems, ultimately disrupting natural

CONTACT Shanker Lal Meena slmeena.jnvu@gmail.com Department of Chemistry, Jai Narain Vyas University, Jodhpur, Rajasthan, India.

Doi: http://dx.doi.org/10.12944/CWE.20.3.23

oxygenation and damaging aquatic life.[1-2] Chemical oxidation methods, including chlorination, have been reported to produce hazardous by-products like organochlorine compounds, thereby raising secondary pollution concerns.[3-4] Similarly, photo-oxidation processes, although effective, frequently necessitate additional chemical inputs, which also contribute to pollution. Biological degradation shows limited success due to the inhibitory effects of dye toxicity on microbial activity.[5]

Advanced Oxidation Processes (AOPs) have gained significant attention as promising alternatives for azo dye degradation. AOPs operate by generating potent oxidizing radicals, including hydroxyl and superoxide anions, capable of breaking down the stable azo bonds in these dyes selectively and efficiently.[6-11] Among AOPs, heterogeneous photocatalysis stands out as a cost-effective and environmentally benign technique. This process involves the excitation of semiconductor photocatalysts under UV light, leading to the creation of electron-hole pairs. These charge carriers react with dissolved oxygen and water to form reactive oxygen species that attack and degrade dye molecules, ultimately mineralizing them into harmless inorganic substances like carbon dioxide and water.[12-17]

Recent advancements have focused on enhancing photocatalytic efficiency by immobilizing catalysts on supports, improving solar energy utilization, and increasing surface area for adsorption and reaction. For example, Methylene Blue Immobilized Resin (MBIR) Dowex-11 has been extensively studied as an effective photocatalyst for azo dye degradation, demonstrating high removal efficiencies surpassing 95% and following pseudo-first-order kinetics based on Langmuir-Hinshelwood models. The sensitization mechanism and catalyst stability over multiple cycles make MBIR Dowex-11 a practical option for wastewater treatment.[18-23] Meanwhile, Amberchrom 1×2 chloride photocatalysts, which share adsorption and photocatalytic properties due to their immobilized resin structure and fine mesh size, offer similarly promising avenues for dye degradation, albeit with fewer studies reported to date. This current work investigates MBIR Amberchrom 1×2 chloride's application for the photocatalytic degradation of Bismarck Brown Y, addressing this research gap by optimizing parameters such as catalyst dosage, pH, and dye concentration.

This literature synthesis underscores the potential of heterogeneous photocatalysis using immobilized resin photocatalysts like MBIR Dowex-11 and Amberchrom 1×2 chloride, emphasizing their environmental benefits, reusability, and operational feasibility for treating persistent azo dye pollutants.

Properties and Structure

Bismarck Brown Y (BBY) is a frequently found diazo dye, identified by its IUPAC name, 4-[[3-[(2,4-diaminophenyl) diazenyl]phenyl]diazenyl]benzene-1,3-diamine;hydrochloride, and molecular formula (C18H18N8.2HCl) as depicted in Fig.1. The molecular structure of BBY diazo dye encompasses two azo group (-N=N-), four -NH2 groups, with two HCL. When in a solution state, the dye exhibits its λ_{max}. (maximum absorbance) at approximately 463 nm.

Table 1: Properties of Bismark Brown Y Azo dye

Dye Name – Bismarck Brown Y	Appearance – Dark Brown Powder
C.I. Name – Basic Brown 1	Class – Diazo Dye
C.I. Number – 21000	Nature – Basic
Other Name – Manchester Brown, Phenylene Brown	Molecular Mass – 419.3 g mol^{-1}

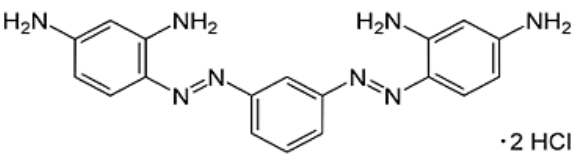

Fig.1: Chemical structure of BBY

Materials and Methods

Materials and Preparation

The substances used in the study, including Bismarck Brown Y (purity = 50%), Amberchrom 1×2 chloride resin (CAS Number – 69011-19-4), Methylene blue dye, HCl, NaOH, and others, purchased from Sigma/ Aldrich company (Saint Louis, MO 63103, USA). The aqueous solutions of above chemical were prepared using double distilled water (ddw).

To prepare a solution of M/500 Azo dye, 0.168g of BBY azo dye was dissolved in 200 ml of double-distilled water. Similarly, for an M/100 solution of Methylene blue, 0.0993 g of Methylene blue was dissolved in 200 ml of ddw. Additionally, 1N solutions of NaOH and HCl were also prepared.

Preparation of Photocatalyst

A solution with an approximate M/100 concentration of methylene blue (MB) was prepared by dissolving it in ddw. Subsequently, Amberchrom 1×2 chloride (100-200 mesh size) resin was incorporated into this solution (1g in 200 ml MB solution) and thoroughly mixed with the help of magnetic stirrer (100 rpm for 30 minutes). The mixture was then left in a dark chamber for 24 hours to allow complete immobilization of methylene blue within the resin pores. Following this incubation period, the methylene blue immobilized photocatalyst was separated from this solution through filtration. The photocatalyst was further washed with ddw and prepared for use as a photocatalyst.

Role of Methylene Blue

Methylene Blue acts as a photosensitizer in photocatalytic processes, absorbing UV light to initiate chemical reactions. When immobilized with Amberchrom 1×2 chloride resin and exposed to light, MB molecules absorb photons and enter an excited electronic state, which facilitates the transfer of electrons. This charge separation results in energized electrons moving to the conduction band and creating corresponding holes in the valence band.

Photocatalytic Activation

Upon excitation, MB enables the generation of key reactive species.

Electrons (e^-) and holes (h^+)

These fundamental charge carriers are produced as MB transitions to its excited state, allowing for subsequent redox reactions.

Hydroxyl Radicals ($OH^•$)

The holes (h^+) generated can react with water or hydroxide ions to produce highly oxidative hydroxyl radicals, which are instrumental in degrading organic pollutants.

Superoxide ions (O_2^-)

The excited electrons can reduce dissolved oxygen to form superoxide ions, contributing further to the oxidative potential of the system.

Role in Photocatalysis

Initiates Charge Separation

MB's role is to absorb UV light and facilitate the separation of charge, producing electron-hole pairs essential for subsequent oxidizing reactions.

Generates Reactive Oxygen Species

The excited electrons and holes evoke redox processes that yield reactive oxygen species, such as hydroxyl radicals and superoxide anions, which are crucial for the breakdown of contaminants.

Enhances Oxidative Efficiency

By being immobilized on a solid resin, MB increases the efficiency, stability, and reusability of the photocatalytic system, while also improving the generation of oxidative species for pollutant removal.

In summary, methylene blue acts as a key driver in photocatalytic activity by absorbing light, promoting charge separation, and triggering the formation of highly oxidative species, all of which contribute to the degradation of azo dye in solution (Fig.2).[24-25]

Characterization Methods

The samples were characterized using various instruments, including a FTIR- ATR Spectra (Thremo Scientific, NICOLET, iS50 FT-IR) Tri-detector, with a scanning range (400-4000 cm^{-1}), a UV Visible Spectrophotometer (SYSTRONICS 2202, double beam), and a JSM-6390 SEM (Jeol USA, Inc.). The UV–Visible spectrophotometer (CSIM-500 microprocessor) was utilized to measure the respective solutions.

Photocatalytic Degradation Experiment

In the photocatalytic degradation of BBY, 0.25g of Amberchrom 1×2 chloride resin was immobilized with methylene blue (M/100 solution in double distilled water) for 24 hours in a dark chamber for the

preparation of photocatalyst. After the 24 hours, the immobilized photocatalyst was filtered and washed with double distilled water. Photocatalytic degradation experiments were conducted in a photoreactor containing a solution of BBY and the photocatalyst. The BBY azo dye and photocatalyst solution were consistently stirred using a magnetic stirrer (100 rpm) throughout the experiment. An exhaust fan was used to remove extra heat (to maintain 300C) from the photoreactor box. The solution was illuminated above the photoreactor with the source of UV LED lamp (Figure 3). Aluminium reflectors were used to surround the radiation lamp, preventing any loss of radiation. After every 5 minutes, the absorbance of BBY azo dye solution with photocatalyst was recorded with the help of UV-Visible spectrophotometer. Photocatalytic degradation under UV LED lamp involves the activation of oxygen species and electron excitation processes, which mainly target dye molecules and trigger their breakdown through photocatalysis.

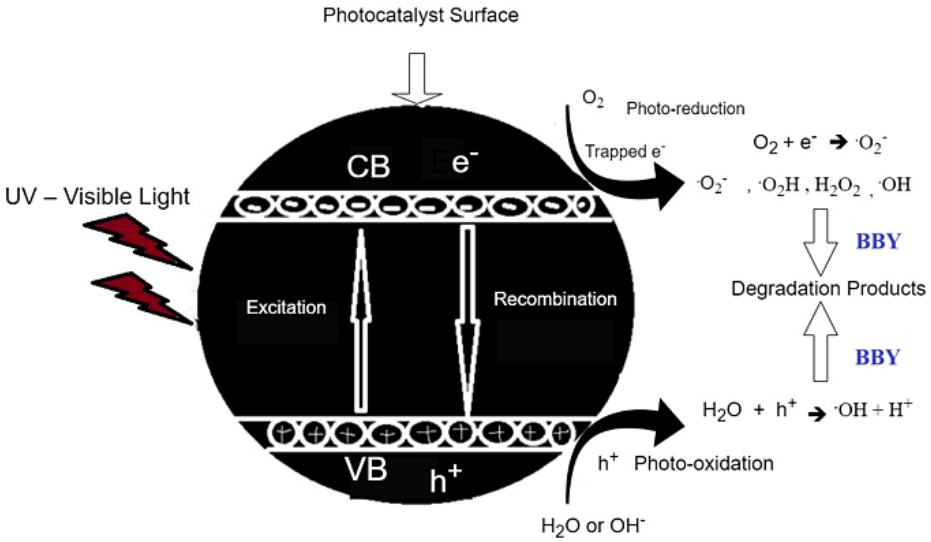

Fig. 2: Schematic diagram of the photocatalytic dye degradation mechanism

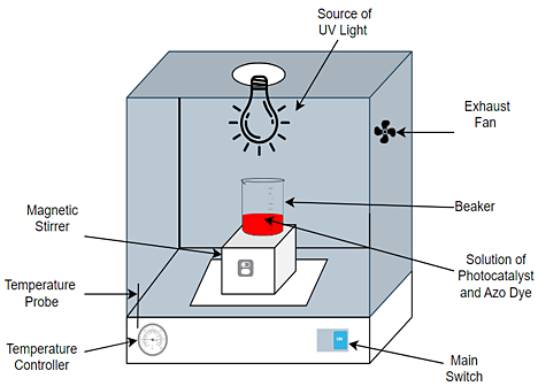

Fig. 3: Schematic diagram of the experimental setup

The absorbance (A_t) at time (t) was compared with the absorbance of the initial solution of BBY azo dye (A_o) which corresponds to the initial (C_o) and final (C) concentrations of BBY in milligrams per litre (mg/L). This comparison allowed for the assessment of the extent of Azo dye photocatalytic degradation (η) using the formula provided in references.[26-28] The photocatalytic degradation efficiencies were calculated as averages based on triplicate measurements.

$$\eta\ (\%) = [(C_o - C)/C_o)] \times 100 = [(A_o - A_t)/A_o)] \times 100$$

Result

Characterization Studies

ATR-FTIR Studies

A comparative ATR-FTIR spectroscopic study of the before (4a) and after (4b) degradation samples reveals significant information regarding the status of the azo bond (–N=N–) within the compound.

Comparative Analysis of FTIR Spectra

Presence of Azo Bond Before Degradation (4a)

- In spectrum (4a), the region from 1400–1600 cm-1 displays a series of broad, moderately intense peaks.
- This area commonly represents the stretching vibrations of the azo group (–N=N–) as well as aromatic C=C bonds.
- The presence of these features is an indicator that the azo functionality is intact in the original, undegraded sample.

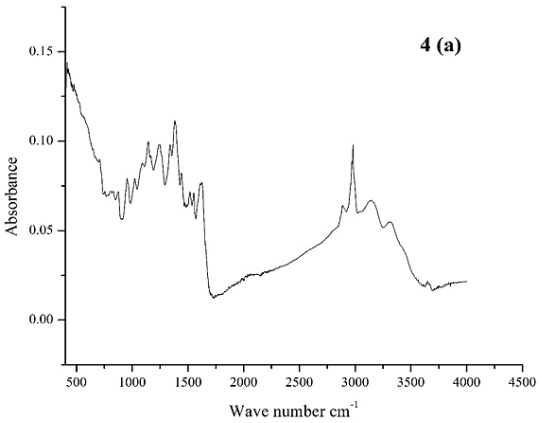

Fig. 4a : FTIR Spectra of BBY azo dye before degradation.

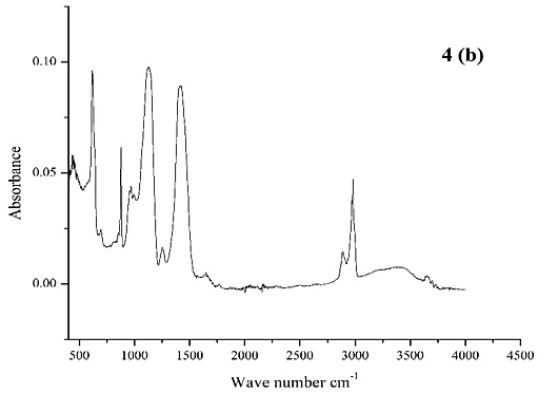

Fig. 4b: FTIR Spectra of BBY azo dye after degradation.

Spectral Changes After Degradation (4b)

- After degradation (4b), the pattern in the 1400–1600 cm-1 region changes markedly: the broad bands observed previously are replaced by several sharp, well-defined peaks.
- Such transformation suggests the disappearance or modification of the azo group, most likely due to bond cleavage or chemical conversion during degradation.
- New peaks emerging below 1500 cm-1 may correspond to new functional groups or by products formed from the breakdown of the original azo structure.

Other Observations

- The region around 3000 cm^{-1}, often associated with C–H stretching vibrations, remains relatively consistent in both spectra, indicating that alkyl or aromatic hydrogen environments are still present after degradation.
- The pronounced spectral changes in the fingerprint and azo-stretch regions provide clear evidence for the disruption of the azo bond upon degradation.[29-30]

SEM Studies

SEM images were employed to observe alterations in the structure and investigation (morphology) of solid surfaces.[31] A comparative analysis of the SEM images (Fig.5a-5c) elucidates the morphological transformations associated with the Bismarck Brown Y azo dye degradation process. Initially, the Amberchrom resin depicted in Figure 5a (Accelerating voltage – 10 kV) displays smooth, well-defined, and nearly perfect spherical particles, attesting to the purity and structural integrity of the fresh resin. Upon immobilization with methylene blue, as observed in Figure 5b (Accelerating voltage – 10 kV), the microspheres retain their overall sphericity, but slight variations in surface texture and a marginal increase in surface roughness are evident, suggesting successful adherence of the dye onto the resin surface without significant agglomeration or structural breakdown. Following the degradation of Bismarck Brown Y, the surface morphology, as shown in Figure 5c (Accelerating voltage – 15 kV), undergoes a profound transformation—distinct spherical forms disappear, replaced by irregular, porous, and highly aggregated clusters indicative of resin disruption and extensive surface modification due to the dye degradation process. These findings demonstrate a clear progression from ordered resin microspheres through mild modification upon dye immobilization, to dramatic surface restructuring post-degradation, reflecting the substantial morphological impact induced by the interaction with and subsequent breakdown of the azo dye.

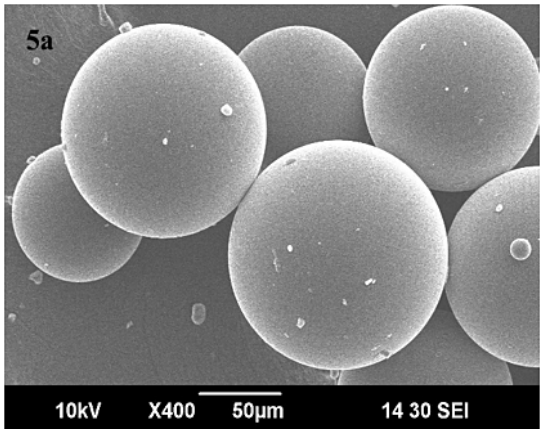

Fig. 5a: SEM image of Amberchrom 1×2 chloride resin.

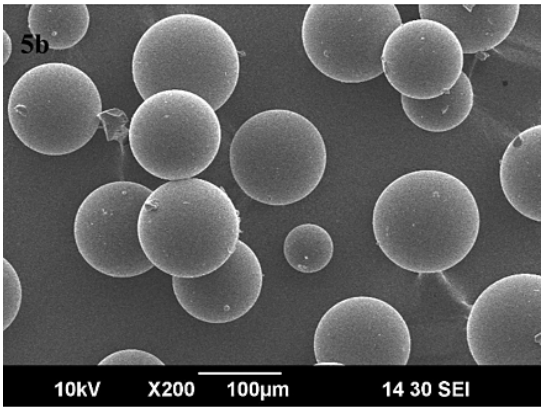

Fig. 5b: SEM image of immobilised Amberchrom 1×2 chloride resin with methylene blue.

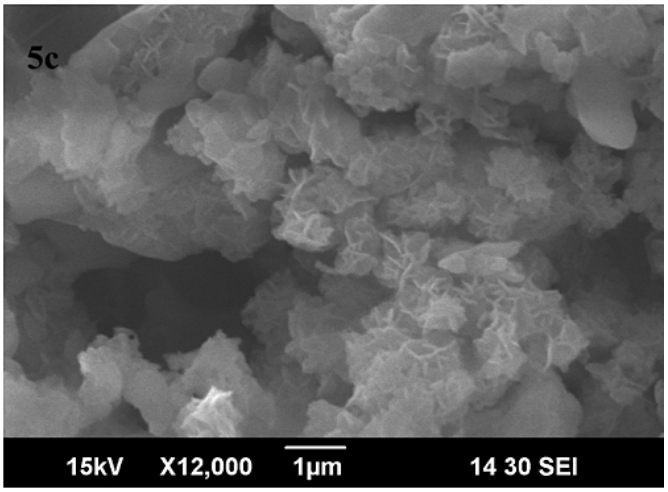

Fig. 5c: SEM image after degradation.

Kinetic Studies

The kinetics of photocatalytic degradation were evaluated to better understand the reaction mechanism and quantify the efficiency of Bismarck Brown Y removal using Amberchrom 1×2 chloride form as the immobilized photocatalyst. Monitoring the absorbance of dye at regular time intervals allowed for fitting the data of pseudo first-order-kinetic model.

Pseudo-First-Order Model

The degradation of azo dyes at low initial concentrations often follows pseudo-first-order kinetics, which is expressed as:

$$\ln(A_o/A_t) = k_{app}\, t$$

$$k_{app} = 1.53\times10^{-1}\,\text{min}^{-1},\ t_{1/2} = 4.53\ \text{min}$$

where A_o and At are the dye absorbance at initial time and time t, respectively, and k_{app} is the apparent first-order rate constant. A linear plot of $\ln(A_o/A_t)$ versus time (t) indicates pseudo-first-order behavior (Fig. 6), and the slope yields the rate constant. The determined R^2 value of 0.994 for the linear fit demonstrates a very strong correlation between $\ln(A_o/A_t)$ and time, validating the appropriateness of the first-order kinetic model for the data.

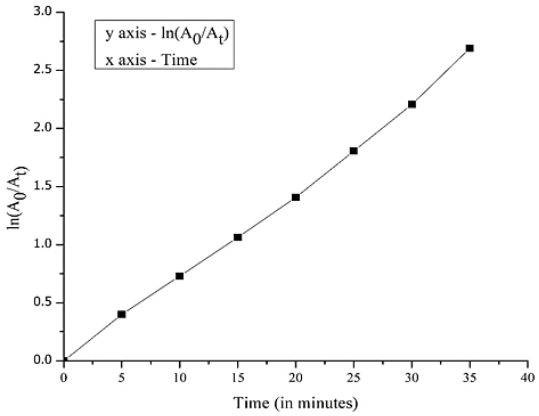

Fig. 6: Linear plot of ln(A_0/A_t) versus Time (t)

UV -Visible Studies

The UV-visible spectrum of Bismarck Brown Y azo dye exhibits a characteristic absorbance curve stretching from 250 nm to 600 nm, with its most pronounced peak at 463 nm (Fig. 7). This intense band at 463 nm is typical for azo dyes and results from strong electronic transitions associated with the dye's chromophore structure. At wavelengths below 300 nm and above 550 nm, absorbance remains low, while the peak region reflects the dye's high affinity for absorbing visible light, making it highly responsive in spectrophotometric and photocatalytic studies. The smoothly varying profile demonstrates Bismarck Brown Y's effectiveness in applications that use visible or UV light for analysis and degradation processes.

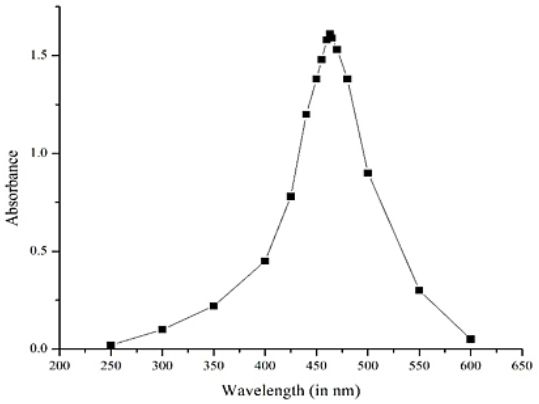

Fig. 7: UV-Visible spectra of BBY azo dye

Photocatalytic Studies

Effect of Photocatalyst Dosage

In the photocatalytic degradation process, the overall yield was significantly influenced by factors such as the scattering of photons from the solution, the effective photocatalyst surface area (which depended on the degree of aggregation of the photocatalyst species), and the number of effective active sites within the reaction chamber. The effectiveness of these factors was contingent upon the dose of the photocatalyst applied. At a low dose (0.25 g), the available active sites were insufficient to serve as active centres for absorbing the incoming photons. Consequently, an increase in the dose (0.25 g to 0.40 g) was anticipated to expose more active centres to the photons, generating additional e-/ h+ and other reactive species, increase in photocatalytic degradation (Fig.8). However, once the optimal dose was surpassed, aggregation of the catalyst species reduced the effective surface area. Moreover, a substantial portion of the incoming photons could be scattered by the high concentration of solid species, resulting in decreased activity once the optimum dose was exceeded.

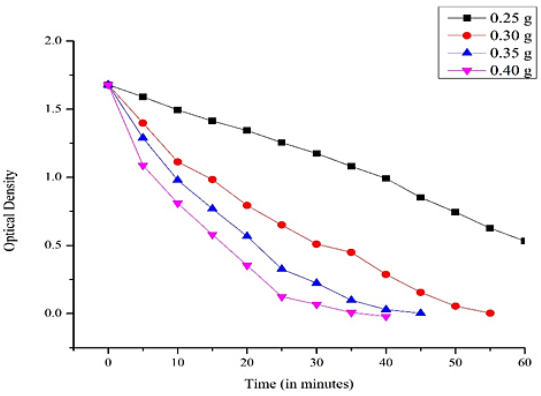

Fig. 8: Comparison diagram of photocatalytic dye degradation with different photocatalyst dosage.

Effects of Neutrality, Alkalinity, and Acidity (pH)

This study investigated the effect of pH on the photocatalytic degradation efficiency of BBY azo dye, using immobilized Amberchrom 1×2 chloride form as the photocatalyst. Experiments were conducted across a range of pH values (3.2–11), while maintaining consistent dye concentration (40mg/L) and catalyst loading (0.25g). Results showed that degradation efficiency improved as the pH became more alkaline, with the highest rate observed at pH 11 (Fig. 9). The enhanced performance at elevated pH was attributed to increased hydroxide ion concentration,

which facilitated the generation of hydroxyl radicals—key oxidizing species responsible for dye breakdown. These findings underscore the importance of optimizing pH conditions in wastewater treatment processes for effective removal of azo dyes, highlighting the dual influence of pH on dye speciation and catalyst surface charge.

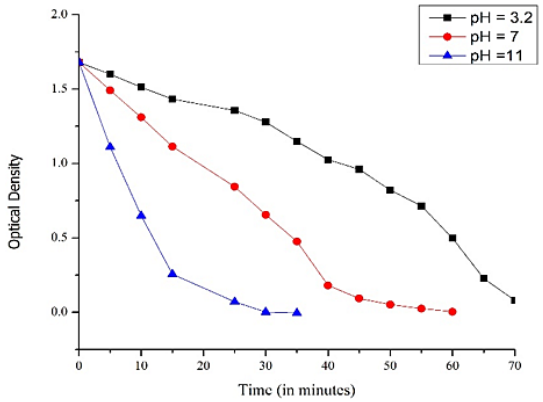

Fig. 9: Comparison diagram of photocatalytic dye degradation at different pH.

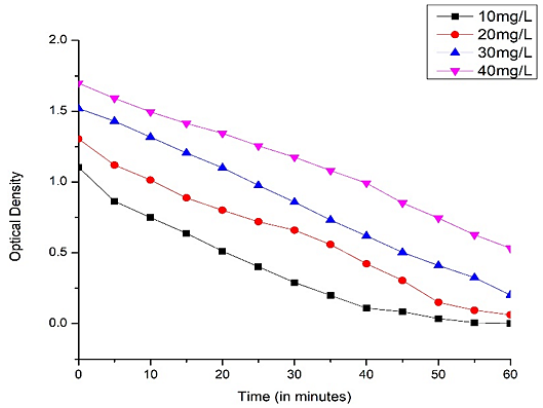

Fig. 10: Comparison diagram of photocatalytic dye degradation with different dye concentrations.

Effects of BBY Dye Concentration

Once the pH conditions and photocatalyst dose were optimized, the photocatalytic degradation of BBY azo dye was conducted. The initial BBY dye concentration (10-40 mg/L) to evaluate with the appropriate photocatalyst dose (0.25g). With an increase in the concentration of BBY azo dye, the percentage of photocatalytic degradation decreased, signifying the necessity to either augment the photocatalyst dosage or prolong the time for a thorough removal. Figure 10 illustrated the optical density V/s time graphs of photocatalytic degradation of BBY azo dye at different concentrations of BBY dye solution (10–40 mg/L). The observed behaviour can be elucidated by the increase in BBY dye concentration, resulting in a reduction of the path length of photons entering the solution. Conversely, lower concentrations exhibited a different effect, leading to an increased number of photons being absorbed by the photocatalyst.

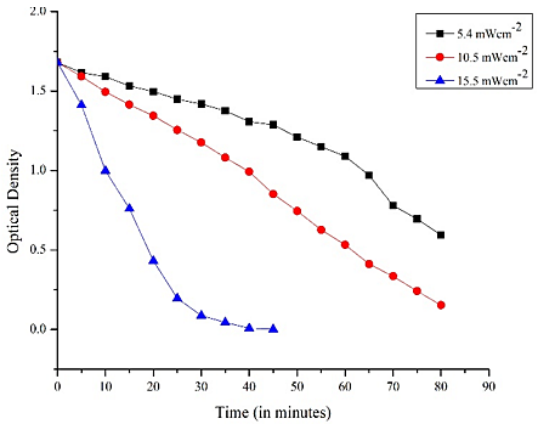

Fig. 11: Comparison diagram of photocatalytic dye degradation with different light intensities.

Effects of UV Light

The speed of the photocatalytic reaction was substantially affected by the absorption of radiation by the photocatalyst. An increase in the degradation rate with a rise in light intensity during the photocatalytic degradation. The reaction pathway remained unaffected by the nature or form of light. The impact of light source on degradation of BBY dye was investigated at a pH (7) and a photocatalyst dose (0.25g) for 1 hour. The impact of UV light was evaluated by adjusting the UV LED lamp source output to 5.4 $mWcm^{-2}$, 10.5 $mWcm^{-2}$, and 15.5 $mWcm^{-2}$ (Figure 11). As anticipated, the data demonstrated that for both factors, the removal efficiency escalated with higher light radiation, resulting from the increased formation of electrons and holes. UV irradiation generated the essential photons for electron transfer from the valence band (VB) to the conduction band (CB) of a photocatalyst. The energy of the photons was associated with their wavelength, and the total energy input to the photocatalytic process

was contingent on light intensity. The degradation efficiency increased as a greater amount of radiation reached the photocatalyst surface, leading to the production of extra hydroxyl radicals.

Effects of Photocatalyst Reusability

The reusability of the immobilized Amberchrom photocatalyst for the degradation of BBY was examined under the same conditions used in Figure 12. After each cycle, the catalyst was separated, thoroughly rinsed with double-distilled water, and dried at 100 °C for 10 minutes before reuse. As shown in the chart, the photocatalyst maintained a high degradation efficiency of 99%, 98%, 97.5%, and 97% over four consecutive cycles (Cycle 1–4), indicating excellent stability and negligible loss in catalytic performance during repeated use.

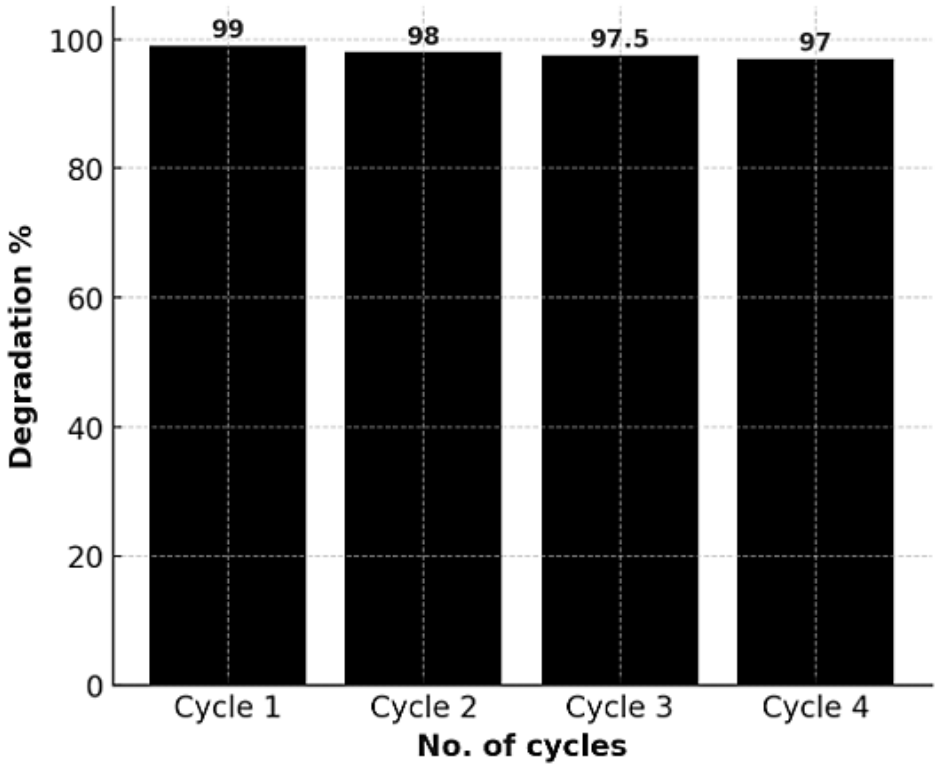

Fig. 12: Recycling runs for photocatalytic degradation of BBY with MBIR Amberchrom 1×2 chloride photocatalyst under the following conditions (Photocatalyst dose: 0.25g, Dye conc.: 40mg/L, pH: 7.0).

Discussion

The findings of this study establish that MBIR Amberchrom 1×2 chloride is an effective heterogeneous photocatalyst for breaking down BBY azo dye. Each parameter tested had a measurable influence on the dye's degradation rate:

Effect of Photocatalyst Dosage

An increase in photocatalyst amount provided a larger surface area and more active sites, leading to greater production of reactive species like hydroxyl radicals and superoxide ions. However, further increases beyond the optimal level showed diminishing returns, possibly due to particle clumping or reduced light penetration.

Effects of Neutrality, Alkalinity, and Acidity (pH)

The degradation process was strongly influenced by the pH of the solution. Enhanced degradation in alkaline conditions is likely due to increased formation of hydroxyl radicals. In contrast, acidic conditions may inhibit this reaction due to excess hydrogen ions interfering with the formation of reactive species.

Effects of BBY dye Concentration

When the dye concentration was higher, the degradation rate decreased. This could be due to the absorption of light by dye molecules themselves, which reduces the number of photons reaching the catalyst surface. Moreover, higher concentrations can saturate active sites, slowing down the degradation process.

Effects of UV Light

As the intensity of light increased, more photons were available to activate the methylene blue in the resin, thus generating more reactive radicals. Nevertheless, once the catalyst was fully activated, additional light intensity did not significantly enhance degradation, indicating a saturation effect.

Effects of Photocatalyst Reusability

One of the key advantages of using MBIR Amberchrom 1×2 chloride is its potential for reuse. After each degradation cycle, the photocatalyst was recovered by simple filtration, washed thoroughly with distilled water, and reused under identical conditions. The photocatalyst retained a significant portion of its activity even after multiple cycles, indicating good stability and sustainability. This reusability makes it a cost-effective and environmentally friendly choice for industrial wastewater treatment.

ATR-FTIR Analysis

Infrared spectroscopy of the treated dye confirmed structural changes, especially the disappearance of the azo group (–N=N–), which is a major contributor to dye toxicity. This confirms the breakdown and detoxification of the dye during photocatalysis.

Conclusion

Synthetic dyes, particularly those released from industries like textiles, leather, and paper, represent a serious environmental hazard due to their persistence, toxicity, and potential for bioaccumulation in aquatic ecosystems. This research investigates the efficient breakdown of BBY, a prevalent azo dye, through photocatalysis using MBIR Amberchrom 1×2 chloride as the catalyst under UV light exposure. The study explores how critical process variables—including pH level, catalyst dose, initial dye concentration, and light intensity—affect the rate and effectiveness of dye degradation (Degradation efficiency = 99.5%). Findings reveal that by fine-tuning these parameters, rapid and nearly complete dye degradation can be achieved within a short irradiation period. The application of UV light, along with the use of a stable and reusable photocatalyst, suggests that this method holds significant promise for cost-effective and scalable treatment of dye-contaminated wastewater. Additionally, the catalyst demonstrates high durability and the ability to be reused across multiple cycles without significant loss of activity. Future investigations should aim to map the degradation pathway of BBY using advanced tools like SEM and ATR-FTIR, which would allow for the identification of intermediate products and confirm the extent of Degradation. Gaining insight into these reaction pathways will be essential for optimizing the process and ensuring its environmental safety, cost effective and efficiency. Conclusion should address broader implications e.g., applicability to real wastewater, cost-effectiveness, comparison to other photocatalysts and limitations.

Acknowledgement

We express our gratitude to the Department of Chemistry at JNVU, Jodhpur for their invaluable support in the successful completion of this work.

Funding Sources

The author received no financial support for the research, authorship, and publication of this article.

Conflict of Interest

The author do not have any conflict of interest.

Data Availability Statement

This statement does not apply to this article.

Ethics Statement

This research did not involve human participants, animal subjects, or any material that requires ethical approval.

Informed Consent Statement

This study did not involve human participants, and therefore, informed consent was not required.

Permission to Reproduce Material from other Sources

Not applicable

Author Contributions

- **Shanker Lal Meena:** Visualization and Supervision
- **Chhatar Pal:** Conceptualization, Methodology, Data Collection, Analysis, Writing Original Draft
- Ashutosh Sharma: Writing – Review and Editing

References

1. Ramos, M. D. N., Cláudio, C. C., Rezende, P. H. V., Santos L. A., Cabral, L. P., Mesquita, P. L., & Aguiar, A. Análise crítica das características de efluentes industriais do setor têxtil no Brasil. *Revista Virtual de Quimica.* 2020; 12:913–929. https://doi.org/10.21577/1984-6835.20200073
2. Tkaczyk, A., Mitrowska, K., & Posyniak, A. Synthetic organic dyes as contaminants of the aquatic environment and their implications for ecosystems: A review. *Science of the Total Environment.* 2020; 717:137222. https://doi.org/10.1016/j.scitotenv.2020.137222
3. Neelakandeswari N, Sangami G, Dharmaraj N, Taek NK, Kim HY. Spectroscopic investigations on the photodegradation of toluidine blue dye using cadmium sulphide nanoparticles prepared by a novel method. *Spectrochim. Acta, Part A*. 2011; 78:1592–1598. https://doi.org/10.1016/j.saa.2011.02.008
4. Masoumi S, Nabiyouni G, Ghanbari D. Photo-degradation of Congored, acid brown and acid violet: photo catalyst and magnetic investigation of $CuFe_2O_4$–TiO_2–Ag nanocomposites. *J. Mater. Sci.: Mater. Electron.* 2016; 27:11017–11033. https://doi.org/10.1007/s10854-016-5218-6
5. Eslami A, Oghazyan A, Sarafraz M. Magnetically separable MgFe2O4 nanoparticle for efficient catalytic ozonation of organic pollutants. Iran. J. Catal. 2018; 8:95–102.
6. Suttikul T, Nuchdang S, Rattanaphra D, Photsathain T, Phalakornkule C. Plasma-assisted CO2 reforming of methane over Ni-based catalysts: Promoting role of Ag and Sn secondary metals. *Int. J. Hydrogen Energy.* 2022; 47:30830-30842.
7. Tran LT, Tran HV, Le TD, Bach GL, Tran LD. Studying Ni(II) adsorption of magnetite/graphene oxide/chitosan nanocomposite. *Adv. Polym. Technol.* 2019; 8124351. https://doi.org/10.1155/2019/8124351
8. Saim AK, Adu PC, Amankwah RK, Oppong MN, Darteh FK, Mamudu AW. Review of catalytic activities of biosynthesized metallic nanoparticles in wastewater treatment. *Environ, Technol. Rev.* 2021; 10:111–130. doi:10.1080/21622515.2021.1893831
9. Cigeroglu Z, Sahin S, Kazan ES. One-pot green preparation of deep eutectic solvent-assisted ZnO/GO nanocomposite for cefixime trihydrate photocatalytic degradation under UV-A irradiation. *Biomass Convers. Biorefin.* 2022; 12:73–86. doi: 10.1007/s13399-021-01734-0
10. Liao M, Su L, Deng Y, Xiong S, Tang R, Wu Z, Ding C, Yang L, Gong D. Strategies to improve WO3-based photocatalysts for wastewater treatment: a review. *J. Mater. Sci.* 2021; 56:14416–14447. https://doi.org/10.1007/s10853-021-06202-8
11. Zhang X, Wei X, Huang SL, Yang GY. Selective photocatalytic oxidation of sulfides in lanthanide metal -organic frameworks incorporating Ru(2,2′ -bpy)3 photosensitizer. *Chem. Asian J.* 2021; 16:2031–2034. https://doi.org/10.1002/asia.202100482
12. Adeyemi JO, Ajiboye T, Onwudiwe DC. Mineralization of antibiotics in wastewater via photocatalysis.*Water Air Soil Pollut.* 2021; 232:219. doi:10.1007/s11270-021-05167-3
13. Sheydaei M, Haseli A, Ayoubi-Feiz B, Vatanpour V. MoS2/N-TiO2/Ti mesh plate for visible-light photocatalytic ozonation of naproxen and industrial wastewater: comparative studies and artificial neural network modelling. *Environ. Sci. Pollut. Res.* 2022; 29:22454–22468. doi:10.1007/s11356-021-17285-w
14. Sabouri Z, Rangrazi A, Amiri MS, Khatami M, Darroudi M. Green synthesis of nickel oxide nanoparticles using Salvia hispanica L. (chia) seeds extract and studies of their photocatalytic activity and cytotoxicity effects,

Bioprocess. *Biosyst. Eng*. 2021; 44:2407–2415. doi:10.1007/s00449-021-02613-8

15. Pourshirband N, Nezamzadeh-Ejhieh A. An efficient Z-scheme CdS/g-C3N4 nano catalyst in methyl orange photodegradation: Focus on the scavenging agent and mechanism. *J. Mol. Liq*. 2021; 335:116543. https://doi.org/10.1016/j.molliq.2021.116543
16. Asadzadeh-Khaneghah S, Habibi-Yangjeh A. g-C3N4 carbon dot-based nanocomposites serve as efficacious photocatalysts for environmental purification and energy generation: A review. *J. Cleaner Prod.* 2020; 276:124319. https://doi.org/10.1016/j.jclepro.2020.124319
17. Sabouri Z, Akbari A, Hosseini HA, Hashemzadeh A, Darroudi M. Eco-friendly biosynthesis of nickel oxide nanoparticles mediated by okra plant extract and investigation of their photocatalytic, magnetic, cytotoxicity, and antibacterial properties. *J. Cluster Sci*. 2019; 30:1425–1434. doi:10.1007/s10876-019-01584-x
18. Meena RC, Pachwarya R, Kumar V. Degradation of textile dyes Ponceau-S and Sudan IV using recently developed photocatalyst, immobilized resin dowex -11. *American J. Environ. Sci.* 2009; 5:444-450.
19. Meena RC, Munesh, Swati. Photocatalytic decolorization of Acid Red 186 using alternative developed photocatalyst mbir dowex 11. Res. *J. Chem. Sci.* 2012; 2:56-62.
20. Swati, Munesh, and Meena RC. Photocatalytic degradation of textile dye through an alternative photocatalyst methylene blue immobilized resin Dowex-11 in presence of solar light. *Archives of Applied Science Research.* 2012; 4(1):472-479.
21. Himakshi, Neelakshi, and Meena RC. MBIR Dowex-11 Assisted Photocatalytic Degradation of Azo Dyes: A Review. *Trends in Scientific Research Journals.* 2017.
22. Kumar, S., and Sharma, A. Studies on Photocatalytic Degradation of Azo Dye Acid Red-18 Using Methylene Blue Immobilized Resin Dowex-11. *International Journal of Engineering and Science.* 2013.
23. Munesh Meena, R.C. Meena. Solar photocatalytic degradation of azo dye ponceau BS through applying alternative developed photocatalyst MBIR Dowex 11. *Trends in Scientific Research Journals.* 2016.
24. Meena RC, Sindal RS, Munesh. Degradation of textile dye from aqueous solution by using mbir dowex photocatalyst. *Int. J. basic and Applied Chemical Sci.* 2012; 2:23-30.
25. Meena SL, Yadav LC, Jaimini H & Meena RC, Degradation of biebrich scarlet textile dye by using mbir dowex-1x8. *Oriental Journal of Chemistry.* 2023; 39:942- 947, http://dx.doi.org/10.13005/ojc/390416.
26. Raja VR, Rosaline DR, Suganthi A, Rajarajan M. Facile fabrication of PbS/ MoS2 nanocomposite photocatalyst with efficient photocatalytic activity under visible light. Solid *State Sci.* 2017; 67:99–108. doi:10.1016/j.solidstatesciences.2017.03.016
27. Ranjith KS, Manivel P, Rajendrakumar RT, Uyar T. Multifunctional ZnO nanorod-reduced graphene oxide hybrids nanocomposites for effective water remediation: Effective sunlight driven degradation of organic dyes and rapid heavy metal adsorption. *Chem. Eng. J.* 2017; 325:588–600. https://doi.org/10.1016/j.cej.2017.05.105
28. Yadav LC, Jaimini H, Meena K, Meena RC & Meena SL. Photocatalytic degradation of eriochrome black-t dye by immobilised dowex 1×8. *Research Journal of Chemistry and Environment.* 2023; 27:88-95.
29. Nakanish K, Solomon P (1977) 'Infrared Absorption Spectroscopy', 2nd edn. (Holden-Day, Inc London, Sydeny)
30. Crriddle WJ, Eilis GP (1994) 'Spactral and Chemical Charactreization of organic Compounds', 3rd edn. (Great Britain)
31. Sonu S, Sharma V, Dutta P, Raizada A, Hosseini-Bandegharaei V, Thakur VH, Nguyen Q, P, Singh. An overview of hetero-junctioned $ZnFe_2O_4$ photocatalyst for enhanced VanLe oxidative water purification. *J. Environ. Chem. Eng.* 2021; 9:105812. https://doi.org/10.1016/j.jece.2021.105812